AD_____
(Leave blank)

Award Number: **W81XWH-07-1-0716**

TITLE: **Neuroprosthetics and Solutions for Restoring Sensorimotor Function**

PRINCIPAL INVESTIGATOR: Michael Munin

CONTRACTING ORGANIZATION: University of Pittsburgh

Pittsburgh, PA 15260

REPORT DATE: December 2010

TYPE OF REPORT: Annual

PREPARED FOR: U.S. Army Medical Research and Materiel Command
Fort Detrick, Maryland 21702-5012

# REPORT DOCUMENTATION PAGE

*Form Approved*
*OMB No. 0704-0188*



| 1. REPORT DATE *(DD-MM-YYYY)* | 2. REPORT TYPE | 3. DATES COVERED *(From - To)* |
|---|---|---|
| 31-DEC-2010 | Annual | 01 DEC 2009 - 30 NOV 2010 |

**4. TITLE AND SUBTITLE**
**Neuroprosthetics and Solutions for Restoring Sensorimotor Function**

**5a. CONTRACT NUMBER**
W81XWH-07-1-0716

**5b. GRANT NUMBER**

**5c. PROGRAM ELEMENT NUMBER**

**6. AUTHOR(S)**
Douglas Weber, PhD, PI
Carl Lagenaur, PhD, Co-I
Wei Wang, PhD, Co-I
Rory Cooper, PhD, Co-I
Tracy Cui, PhD, Co-I

**5d. PROJECT NUMBER**

**5e. TASK NUMBER**

**5f. WORK UNIT NUMBER**

**7. PERFORMING ORGANIZATION NAME(S) AND ADDRESS(ES)**

University of Pittsburgh
Office of Research
350 Thackeray Hall
Pittsburgh, PA 15260

**8. PERFORMING ORGANIZATION REPORT NUMBER**

**9. SPONSORING / MONITORING AGENCY NAME(S) AND ADDRESS(ES)**
U.S. Army Medical Research
Fort Detrick, Maryland

**10. SPONSOR/MONITOR'S ACRONYM(S)**

**11. SPONSOR/MONITOR'S REPORT NUMBER(S)**

**12. DISTRIBUTION / AVAILABILITY STATEMENT**
Approved for public release; distribution unlimited

**13. SUPPLEMENTARY NOTES**

**14. ABSTRACT**

This project is focused on the development of a radically new class of prosthetic devices that will mimic more closely the full range of sensory and motor capabilities of natural limbs. To this end, we have made initial progress on four integrated projects to advance the development of neuroprosthetic limbs including: 1) creation of a sensory neural interface to provide amputees with tactile and kinesthetic feedback from their prosthetic limb, 2) improving the biocompatibility of implanted neural interface electrodes, 3) development of a virtual reality training and testing system for neuroprosthetic limbs, and 4) development of prosthetic hardware testing equipment and procedures. To date, we have completed pilot experiments to characterize the organization of sensory neurons in the DRG for the creation of a sensory feedback neural interface and evaluated the brain's response to sensory stimulation. We have completed pilot experiments to evaluate histologically the tissue response to electrodes implanted chronically in DRG, dorsal roots, and spinal cord. We have designed and developed a virtual reality training system based on BCI2000, creating custom software to greatly extend the functionality of BCI2000. Finally, we have developed a test jig to determine compliance with ISO standards for prosthetic hardware, and we have begun testing prosthetic feet.

**15. SUBJECT TERMS**
neural interface, neural prosthesis, biocompatibility, virtual reality, amputee, sensory feedback

| 16. SECURITY CLASSIFICATION OF: | | | 17. LIMITATION OF ABSTRACT | 18. NUMBER OF PAGES | 19a. NAME OF RESPONSIBLE PERSON |
|---|---|---|---|---|---|
| a. REPORT | b. ABSTRACT | c. THIS PAGE | | | USAMRMC |
| U | U | U | UU | 33 | 19b. TELEPHONE NUMBER *(include area code)* |

**Standard Form 298 (Rev. 8-98)**
**Prescribed by ANSI Std. Z39.18**

**Introduction**

Advances in body armor and life-saving technology have increased survival rates of severely injured military personnel. Unfortunately, the survivors of improvised explosive devices used in gulf conflicts are often left with amputations and/or spinal cord injuries. The increase in amputations and paralysis among military personnel requires significant advances in prosthetics and functional electrical stimulation (FES) systems such that the soldiers can return to the field if they desire or to productive civilian lives. This project is focused on the development of a radically new class of prosthetic devices that will mimic more closely the full range of sensory and motor capabilities of natural limbs. By providing a communication link between the prosthesis and the user's nervous system, our goal is to integrate the prosthetic limb as a natural component of the user's sensorimotor apparatus. Significant progress has been made toward this goal, but there is still much work to be done, particularly in the areas of restoring sensory feedback, improving the electrode-neuron interface, user-training, and prosthetic durability. **Project 1** deals directly with the issue of providing somatosensory input to soldiers with amputation or paralysis. **Project 2** deals with improving the chronic stability of the neural interface and will test novel polymer surface modification methods for improving the long-term reliability of the implanted microelectrodes. Although neural control is the ultimate goal of our work, we believe that there is useful control information available in the muscles of the residual limb. **Project 3** uses virtual reality to place patients in an environment with a simulated neuroprosthesis. In this environment, we can discover the degree of remaining electromyographic (EMG) signal content and begin to train patients to control their neuroprosthetic. In this way, the virtual environment serves two important purposes: 1) testing algorithms for myoelectric and/or neural control, and 2) training the user on neuroprosthetic control. This new class of prosthetic devices will literally look, feel, and function like natural limbs, but their internal construction will include complex machinery, motors, sensors, and control instrumentation. Therefore, durability is a major concern, especially since users will be more able to engage in rigorous physical activities. Through our interactions with soldiers returning to duty after amputation, we know that current prosthetics do not stand up to the harsh use of active amputees. **Project 4** is designed to rigorously test currently available and newly design prosthetics to understand the components that fail and the ways to remediate these failures. In addition, we will build devices that can track prosthetic use and thus provide information on the use in terms of both distance traveled and force imparted.

## Body

### *Project 1. Develop a somatosensory neural interface (SSNI)*

The overall goal of project 1 is to restore natural sensations of limb posture and movement through multichannel microstimulation of the normal afferent pathways involved in proprioception. Two objectives must be met to achieve this overall goal. First, we must identify an appropriate location in the somatosensory nervous system for implanting microelectrode arrays to stimulate primary afferent (PA) neurons. We are examining the somatotopic organization and recruitment of primary afferent fibers in the DRG, dorsal root, and dorsal root entry zone to develop a technique called primary afferent microstimulation (PAMS). Multichannel PAMS is used to generate a spatiotemporal pattern of sensory input that encodes limb-state information for the whole limb. Neural recordings in primary somatosensory cortex are used to evaluate the response in the brain, and evaluate the effectiveness of various inputs.

In the first year of this project, we characterized the stimulation threshold for recruiting PA fibers (Gaunt, 2009). We have also developed a computational model to provide a theoretical framework for further exploration (Bourbeau, 2011 in review). In addition, we are continuing to perform studies to evaluate the brain's response to PAMS (Weber, 2011 in preparation). This portion of animal testing was performed in conjunction with a related NIH funded project. We will be starting the TATRC-funded cat studies this year. We have recently obtained approval from our local IACUC and the Army ACURO to perform the cat studies.

A summary of the results obtained over the last year and plans for further testing in the coming year are provided below. Briefly, our modeling studies have provided some very interesting insights into the nature of sensory fiber recruitment by PAMS in the dorsal root ganglia (DRG). Notably, the model shows that PAMS is highly selective for activating smaller diameter fibers, whereas other techniques tend to recruit only the large diameter fibers. This finding is extremely important, because it further demonstrates that our approach will be useful for activating specific cutaneous and muscle afferent fibers as needed to restore touch and proprioception. In the coming year, we will begin evaluating this approach in chronically implanted animals to evaluate the quality and stability of sensory inputs provided by PAMS (see 'Plans' section).

#### *Results: A computational model to characterize recruitment of PA neurons by microstimulation in the DRG*

Electrical stimulation of peripheral nerve fibers holds great potential for developing motor and sensory neural prostheses. Selective activation of different sensory fiber types is important for the development of a somatosensory neural interface (SSNI) for restoring tactile and proprioceptive sensations for neuroprosthetic limbs. Specifically, microstimulation of PA fibers in the dorsal root ganglia (DRG) is being explored as a means of providing tactile and proprioceptive feedback. A sensory neural interface comprising electrodes in a few DRGs could provide access to the full range of somatosensory fibers covering large portions of a limb in a compact and mechanically stable structure. Previously, we performed primary afferent microstimulation (PAMS) studies with penetrating microelectrodes in the DRG to determine the electrical current thresholds for activating PA fibers. The conduction velocities of fibers that were recruited at the lowest thresholds varied from 38-118 m/s, indicating that a wide range of fiber diameters were recruited in isolation. The diameters of these fibers corresponded to Aalpha and Abeta cutaneous afferents, and group I and group II muscle afferents. The thresholds for all of these fibers were similar, typically 1-3 μA (Gaunt, Hokanson et al. 2009). This pattern of neutral recruitment order has also been observed with intrafascicular electrodes in the peripheral nerve, and suggests that at low intensities, fibers located nearest the electrode can be recruited selectively, independent of fiber diameter. Such selective recruitment would be particularly advantageous for creating a SSNI, where it is

desirable to activate fibers of various types to transmit specific modes (e.g. tactile and proprioceptive) of somatosensory feedback.

Computational models have provided valuable insight into the effects of electrical stimulation on fiber recruitment in peripheral nerves. Previous models were based on specific geometries for the fiber bundles and do not generalize easily to other structures. In particular, the irregular and variable arrangement of fibers and cell bodies in the DRG make it impractical to define a specific geometry to model the various electrode-fiber configurations that are possible. An alternative approach, which has been used for modeling the recruitment of fibers by deep brain stimulation (DBS), is to estimate the volume of tissue activated (VTA) by a given stimulus current. The VTA is defined by the current-distance relation for each fiber diameter, which predicts the activation threshold as a function of the distance between the current source and nearest node of Ranvier. Thus, a given stimulus will activate all fibers having at least one node within the boundary of the VTA.

The likelihood of activating a fiber of a given diameter can be estimated by determining the probability of capturing a node of Ranvier within the VTA (see Figure 1.1). For a given fiber size, this probability depends on the internodal length as well as the probability of encountering that fiber size within the VTA. We implemented this "likelihood of activation" approach to estimate the recruitment of PA fibers by microstimulation of the DRG. This approach assumes that the distribution of fibers follows published data for the number and distribution of fibers of various diameters in the DRG. We used a multi-compartment neuron model to determine the current-distance relationship for a range of fiber diameters. Given the current-distance relationship for each fiber diameter, the model provides a likelihood estimate of the number and types of fibers recruited based on the density and distribution of fibers by size. These features lead to a flexible model that can simulate various stimulation scenarios and electrode-fiber geometries, including the inhomogeneous distribution of fibers in the DRG.

Activation of a neural fiber depends on several factors, including stimulus waveform and amplitude, fiber size, and distance from the stimulating electrode. Figure 1.2 illustrates the effect of increasing fiber diameter on the current-distance relation, which determines the size of the VTA. In general, the

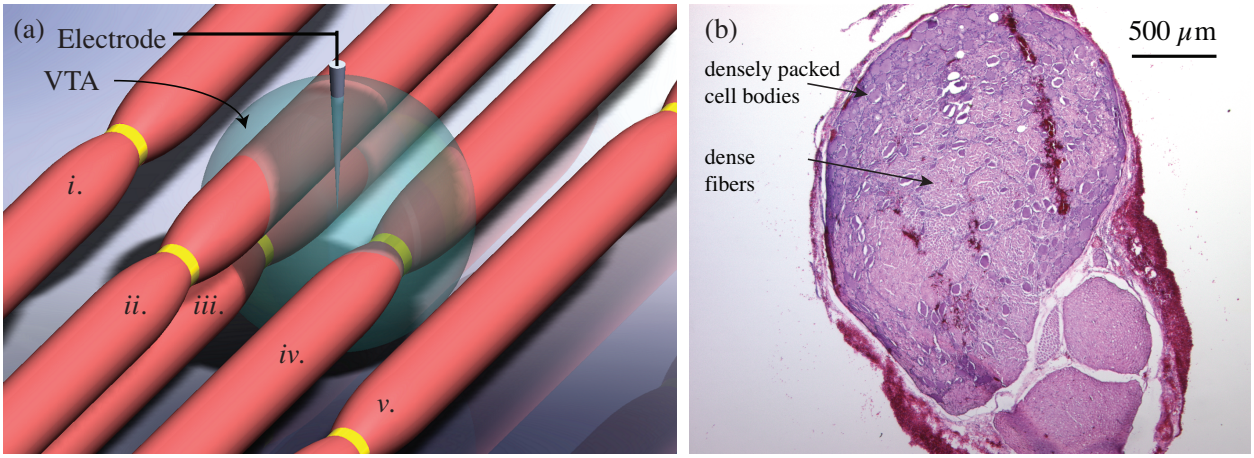


**Figure 1.1**: Sphere representing volume of tissue activated (VTA) by a point-source current stimulus delivered by a microelectrode. (a) The size of the sphere increases with stimulus amplitude and also varies with fiber diameter. The radius is determined by the current-distance relationship calculated with the MRG model for neuronal excitation. Fibers *iii* and *iv*, having a node of Ranvier within the VTA, will be activated. Fiber *ii*, though it passes through the sphere, does not have a node of Ranvier within the sphere and thus will not be activated. Fibers *i* and *v*, likewise, will not be activated. (b) Transverse section of feline L7 DRG (top) and ventral root (bottom), hematoxylin and eosin (H&E) stained. Cell bodies are predominantly located along the perimeter of the DRG, but are also sparsely distributed in the center among fibers of passage in the middle, which results in a heterogeneous tissue structure.

electrode-to-node distance increases with the stimulus amplitude. At higher intensities, the larger diameter fibers can be activated at a much greater distance, or conversely, at large distances (e.g. > 1 mm) the threshold is lower. This gives rise to the so-called 'reverse recruitment' phenomena that has been described for muscle activation with epineural electrodes. However, for amplitudes below 10 µA (see inset in figure 1.2a), there is little difference in the current-distance relationship for fibers of different diameters. Thus, at these low intensities, the radius of the VTA is effectively the same for all myelinated fibers within the range tested. Although the VTA is the same for these fibers, this does not mean that these different sized fibers have equal likelihood of being recruited in the 0-10 µA range. In order for a fiber to become activated, a node of Ranvier must be captured within the VTA.

The model was used to examine the activation of medium (7.3-11.5 µm) and large (12.8+ µm) diameter PA fibers in the feline L7 DRG as a function of stimulus intensity (see Figure 1.3). Simulation results were compared to recruitment data obtained in vivo (Gaunt, Hokanson et al. 2009). Consistent with the in vivo data, the model simulations suggested that medium and large fibers have similar thresholds (~1-3 µA). However, the model simulations revealed a strong bias favoring recruitment of medium fibers, with probabilities of activation more than twice that for the large fibers. The in vivo data showed only a small bias favoring recruitment of medium fibers. Two factors contribute to this bias. First, there are approximately 55% more medium fibers than large fibers, increasing the likelihood of encountering one or more medium fibers in the VTA. Second, the internodal distance is shorter, increasing the likelihood of capturing a node of Ranvier within the VTA. The discrepancy between the simulation results and in vivo data may be due to failure to reliably detect recruitment of individual medium fibers in the in vivo study; it is likely that two or more medium fibers were actually recruited at

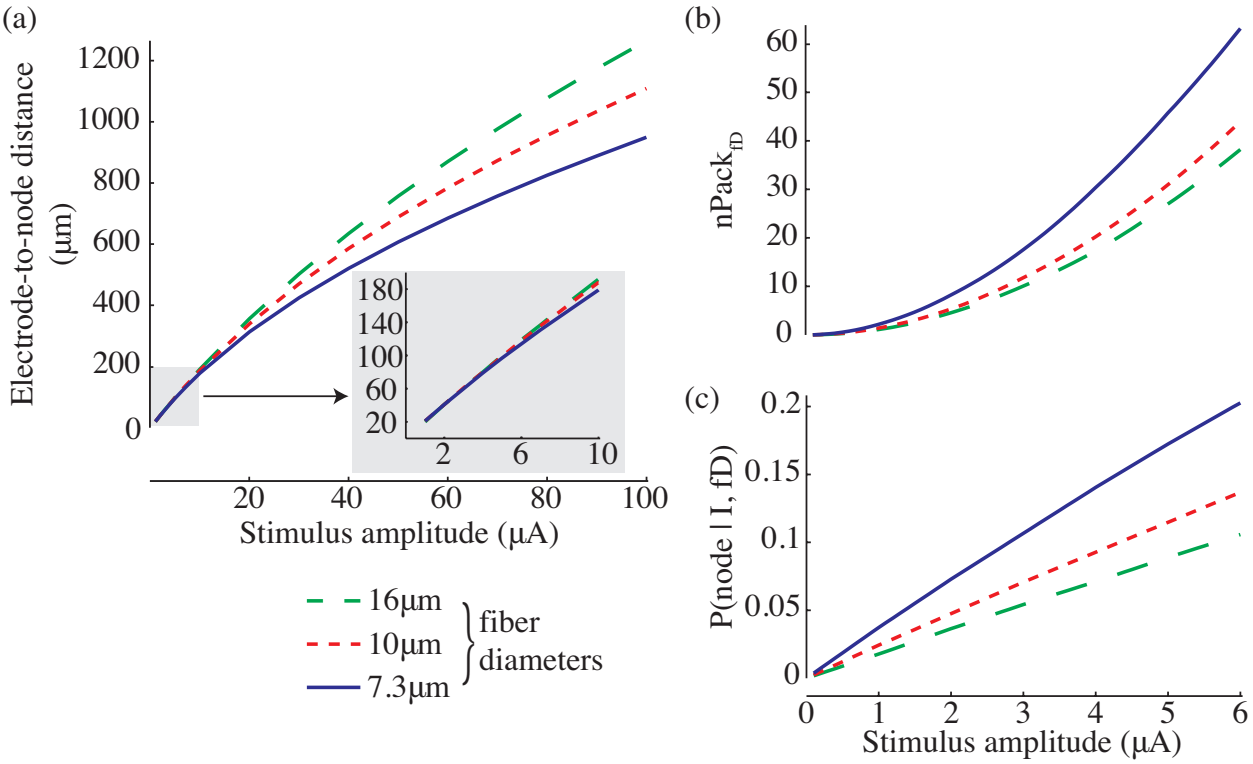


**Figure 1.2:** Effects of fiber diameter on current-distance relation, fiber packing and probability of having a node in the VTA. (a) Current-distance relationships from single-fiber model. Electrode-to-node distance corresponds to the radius of a spherical VTA centered about a stimulating electrode. (b) The number of fibers that can be packed into the VTA assuming a packing ratio equal to 1. (c) Probability of capturing a node of Ranvier in the VTA as predicted by (7). Fiber sizes of 7.3 µm, 10 µm and 16 µm were simulated.

the thresholds found for medium fibers in the in vivo study (see discussion). Finally, the model was used to estimate the number of medium and large diameter fibers recruited by stimulation currents in the range 1-6 A, revealing a slightly sharper rate of recruitment for the medium fibers (see Figure 1.4). We conclude that this probabilistic model is useful for gaining insight into the pattern of sensory fiber recruitment by PAMS in the DRG. This information will be valuable for guiding the design of microelectrode arrays for a SSNI.

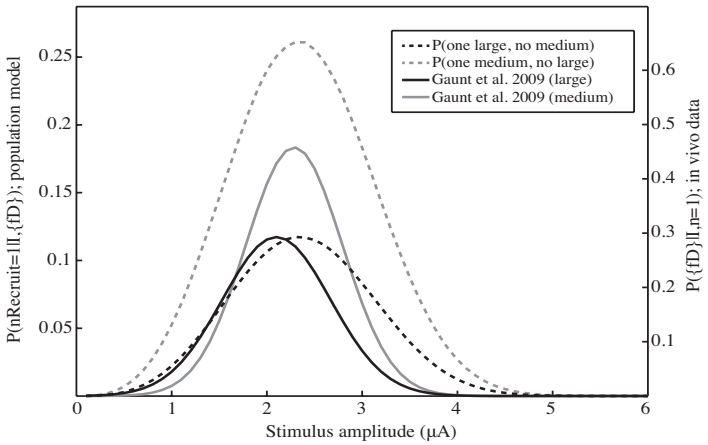


**Figure 1.3:** Comparison of model predictions to electrophysiology data at threshold amplitudes. The solid traces represent the probabilities of recruiting a fiber from one of the two fiber sets {fD}medium and {fD} large, given that a fiber was recruited, as a function of stimulus intensity. The dashed traces represent model predictions for recruiting a fiber from one of the two sets as a function of stimulus intensity. The gray traces represent the probabilities of recruiting exactly one large fiber (12.7-16+ μm). The black traces represent the probabilities of recruiting exactly one medium fiber (7.3-11.5 μm). The y-axis for the model data is on the left and the y-axis for the electrophysiology data is on the right (Gaunt, Hokanson et al. 2009).

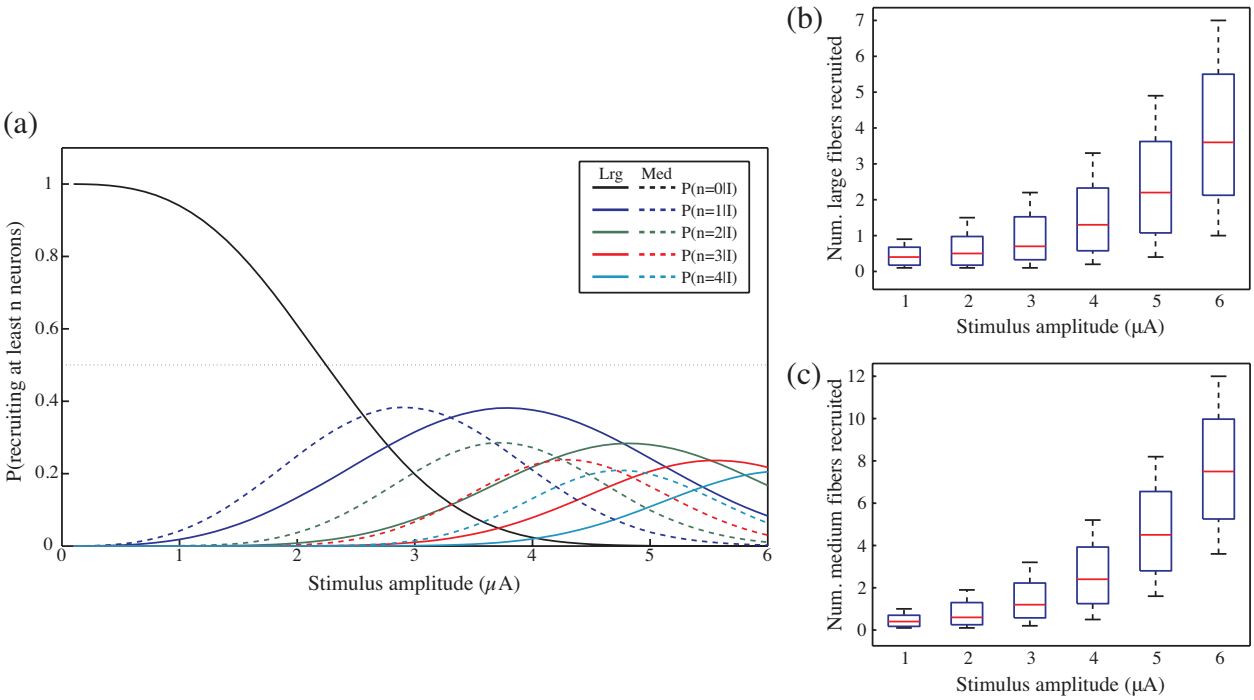


**Figure 1.4:** Recruitment of multiple fibers in a heterogeneous population across stimulation amplitudes in the range 1-6 μA. (a) Traces represent the probabilities of recruiting exactly zero, one, two, three, or four fibers. Solid traces represent recruitment of large fibers (12.8 to 16+ μm) while dashed traces represent recruitment of medium fibers (7.3 to 11.5 μm). (b) and (c) Range of numbers of large and medium fibers recruited, respectively, given stimulus amplitude.

### *Response of S1 to PAMS patterned from neural data recorded during passive movement*

We are developing a somatosensory neural interface (SSNI) for encoding and transmitting tactile and proprioceptive information by primary afferent microstimulation (PAMS) in the dorsal root ganglia (DRG), the effects of which are measured in primary somatosensory cortex (S1). Under normal conditions, the firing rates of PA neurons throughout the limb are modulated during movement, establishing a widely distributed spatiotemporal neural code representing the physical state of the limb. We have developed a 'replay stimulation' paradigm to mimic the global pattern of PA activity produced during movement. Admittedly, the replay pattern is not an exact recreation of the normal PA input, since only a subset (n <= 32 stimulation channels) of the total PA population is activated and may include additional fibers than the ones recorded. By comparing S1 responses to passive movement and replay PAMS, we can gain insight into the amount of movement-related information received in the brain in response to the movement and replay conditions. Further, we can systematically alter the structure (e.g. number and ordering of channels) of replay inputs to examine the effects on S1 responses.

Recordings were made simultaneously in the DRGs and S1 during displacements of the hindpaw. Next, recordings were made in S1 during PAMS (7 & 10 uA) on 30 DRG channels. PAMS pulse patterns on each DRG channel were set to match the spike times recorded during movement trials (i.e. replay PAMS). Extra pulses were inserted on some trials to increase the pulse rate to 4x and 8x the original rate (see Figure 1.5). S1 firing rates were highly correlated with foot speed during movement trials. Linear regression was used to estimate foot speed from firing rates on these 48 channels (R2 = 0.96). Similar models were used to estimate foot speed in replay trials (R2 = 0.40 at the base rate and 7uA). Increasing the replay rate to 4x enhanced the cortical response, yielding a stronger estimate of foot speed (R2 = 0.64), but 8x replay yielded a weaker S1 response (R2 = 0.43). This trend was also observed at 10 uA with R2 values of 0.60, 0.76, and 0.58 for 1x, 4x, and 8x respectively.

These results show that PAMS with only 30 channels is effective at evoking neural responses in S1 that are similar to those evoked by whole limb movement. Further, amplifying the stimulation pulse rate can enhance the cortical response, but the range of pulse rates may be limited. By using higher than normal pulse rates, we hypothesize that temporal summation at downstream synapses may partially compensate for the limited number of input channels. The use of replay stimulation and its variants provide a basis for examining the use of PAMS in providing proprioceptive feedback.

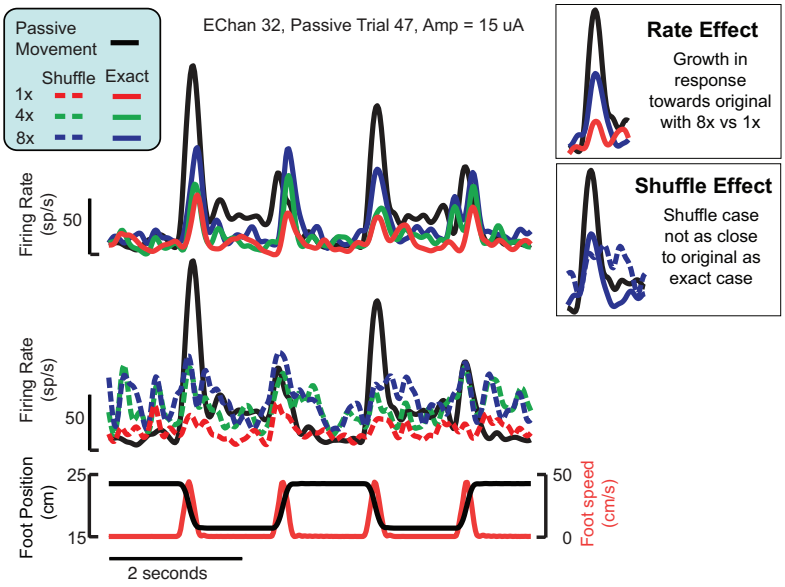


**Figure 1.5:** Stimulation pulse rate and channel shuffle effects. The example shows the cortical response (firing rate) of a single channel to passive movement and 1x, 4x, and 8x replay stimulation rates (top) and channel shuffles (below). Increasing the stimulus pulse-rate shows an increased cortical response during the exact match case.By shuffling stimulus channels the signal degrades, showing that the response is not merely a result of the aggregate stimulation rate.

### *Effects of PAMS rate and amplitude on S1 response*

To develop a more fundamental understanding of the effect of PAMS on S1 responses, we have begun to investigate the effect of varying the rate, intensity and spatial location of

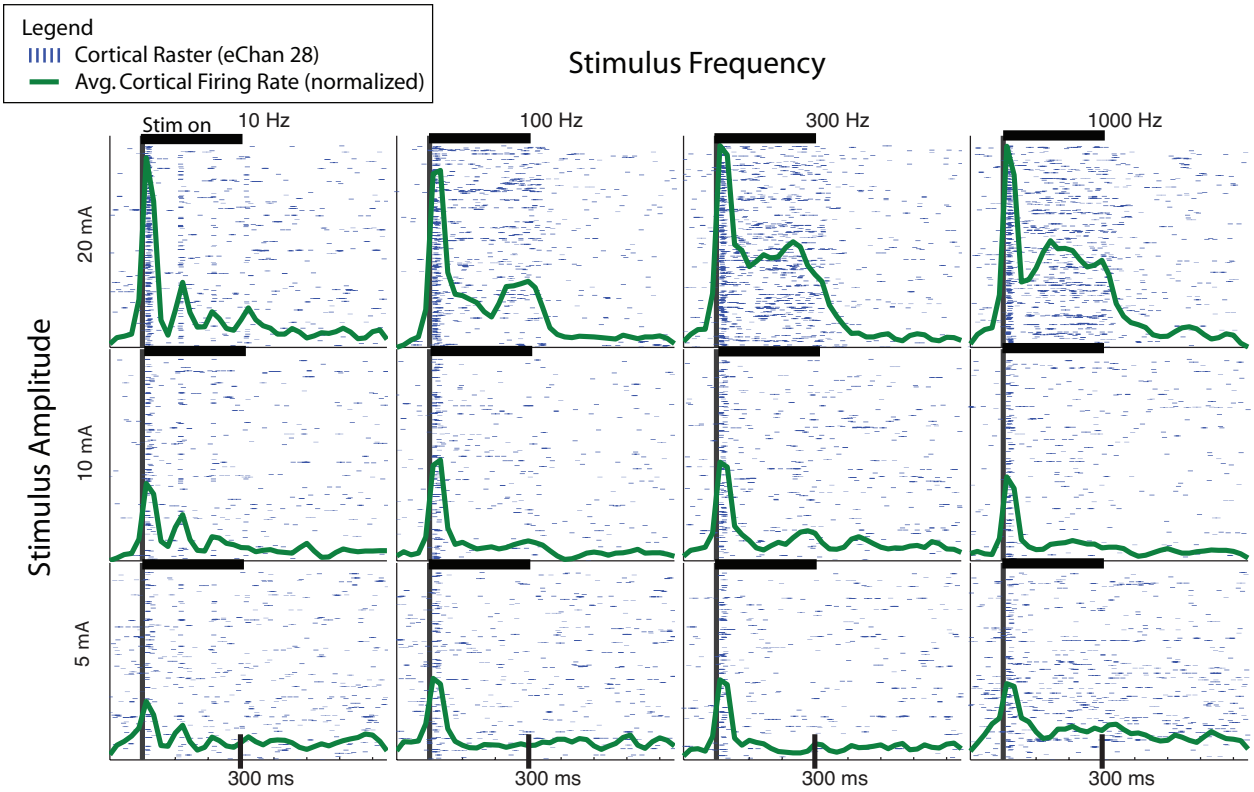


**Figure 1.6:** Stimulus aligned spike rasters and smoothed firing rates from a single cortical channel. All 30 stimulus channels are randomly interleaved for each condition (frequency/amplitude pair). A strong onset response is seen, that increases with increasing amplitude.

single- and paired-channel DRG stimulation. Utah arrays were placed in the L6 (4x10 array) and L7 (5x10 array) DRG and hindlimb region of somatosensory areas 3a and 3b in an anesthetized cat. Stimulus pulses (200 us cathodic phase followed by 400 us anodic phase) were generated on various combinations of one or two DRG electrodes with amplitudes of 5, 10 or 20 µA at pulse rates of 10, 100, 300 and 1000 per second with each stimulus train lasting 500 ms.

Stimulation at 5 µA (all frequencies) resulted in an increased firing rate in 18 ± 16% of the cortical electrodes in the 10 - 60 ms post-stimulus onset window whereas stimulation at 10 µA and 20 µA increased the firing rate on 29 ± 15% and 41 ± 18% of the electrodes respectively. At 5 and 10 µA, but not 20 µA, there was an adaptation in the S1 responses over the duration of the stimulus train with nearly half of the channels showing a reduction in firing rate after the onset response during the 210 - 260 ms post-onset window. However, dual channel stimulation tended to prolong the S1 response into this later time window, even when the stimulation amplitude was low (5 µA). Frequency had no effect on the number of cortical channels exhibiting an onset response, but higher frequencies of stimulation (100 Hz) tended to prolong the onset response on several channels.

***Plans***

We plan to begin testing the proposed PAMS method for providing somatosensory feedback in chronically implanted animals in March, 2010. The IACUC and ACURO protocols have been approved and we are currently ordering the supplies needed for the chronic implant surgeries. We have started training the animals to behave appropriately during the stimulation experiments. Cortical recordings will be made via a skull mounted chamber installed over primary somatosensory cortex, allowing reliable access for placement and manipulation of microelectrodes in primary somatosensory cortex. These

studies will support the year 2 objectives, which are to evaluate 1) the amount of limb-state information that can be delivered to the brain by PAMS, and 2) reliability of this approach over an extended implant period (up to 6 months).

***Project 2. Establishment of Neural interface stability and optimization***

The implanted neural interface must remain stable throughout the lifespan of the user, but immune and inflammatory reactions at the implant site are known to degrade the performance of implanted microelectrodes. Since tissue reactions vary in different parts of the nervous system, our objectives are 1) to examine the tissue responses around electrodes implanted in the DRG and spinal cord 2) to test whether surface coating, with agents that encourage specific neuronal survival and growth and reduce inflammation, will be effective in improving the biocompatibility and 3) to examine the effect of chronic stimulation on surrounding tissue. In the first two years of the project, we have optimized the probe implantation, tissue processing and quantification protocols, developed neuron promoting L1 coating and electrically controlled dexamethasone release coatings. In the past year, we have completed the chronic implantation and histology study. Extensive characterization of the cellular tissue response around the electrodes in DRG and SC at both acute and chronic time points are performed. The effect of the L1 coating was evaluated in vivo, and encouragingly the L1 coating showed trends of reduced microglia/ macrophage activation and kill zone size. A novel PEDOT/carbon nanotube coating was developed for the stimulating electrodes. This coating can be directly deposited on the electrode sites and improve the impedance and charge injection capacity of the electrodes by several orders. Such properties are expected to induce less tissue damage caused by chronic stimulation. In addition, anti-inflammatory drug can be released during the stimulation to further protect the neurons and reduce scarring. Below is detailed report on these results.

***Result 1: Characterization of the tissue responses around neural electrodes in DRG and spinal cord on uncoated and L1 coated probes***

The reactions to the implanted electrodes for the DRG and SC can be observed in Figures 2.1 and 2.2, respectively. Both tissues reacted similarly to the electrodes and to the L1 coating in that there were cells aggregated and oriented around the electrode-tissue interface. More specifically, Iba-1 staining in both the DRG and SC was more intense around the electrode implantation site and decreased in intensity farther from this interface. Conversely, the NF-200 staining in both tissues was decreased or absent in the area immediately surrounding the implant, an area termed the "kill zone". Neuronal process and cell body staining were evident outside of this area in both DRG and SC.

In comparing the uncoated and L1-coated electrodes, two phenomena were observed. First, the L1 coating was associated with a decrease in the inflammatory reaction as characterized by Iba-1 staining (Figures 2.1 and 2.2, green fluorescence). In addition, the degree of NF-200 staining was significantly increased in the presence of L1-coated electrodes (Figures 2.1 and 2.2, red fluorescence). More specifically, the area lacking NF-200 staining around the electrode (the "kill zone") was decreased in size with L1-coated electrodes. These differences suggest that the L1

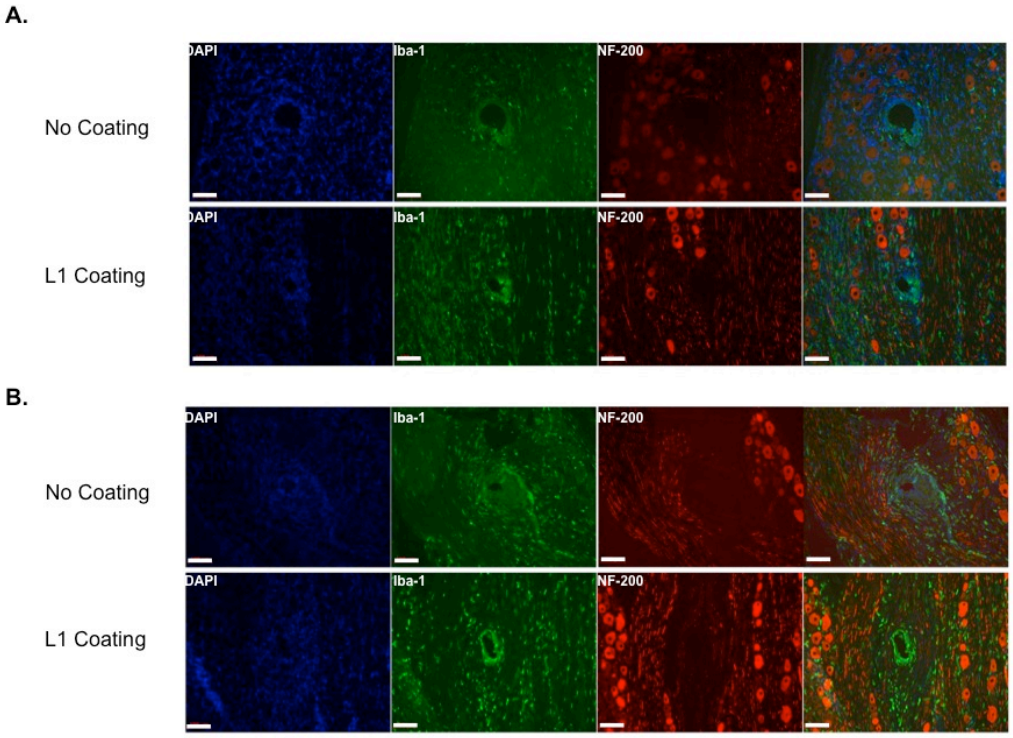


**Figure 2.1**. Immunofluorescence images of rat DRG around uncoated and L1-coated electrodes. **A**: After 1 week, Iba-1 staining was decreased in L1 coated electrodes. **B**: After 4 weeks, this difference was more pronounced. Scale bar represents 100 µm.

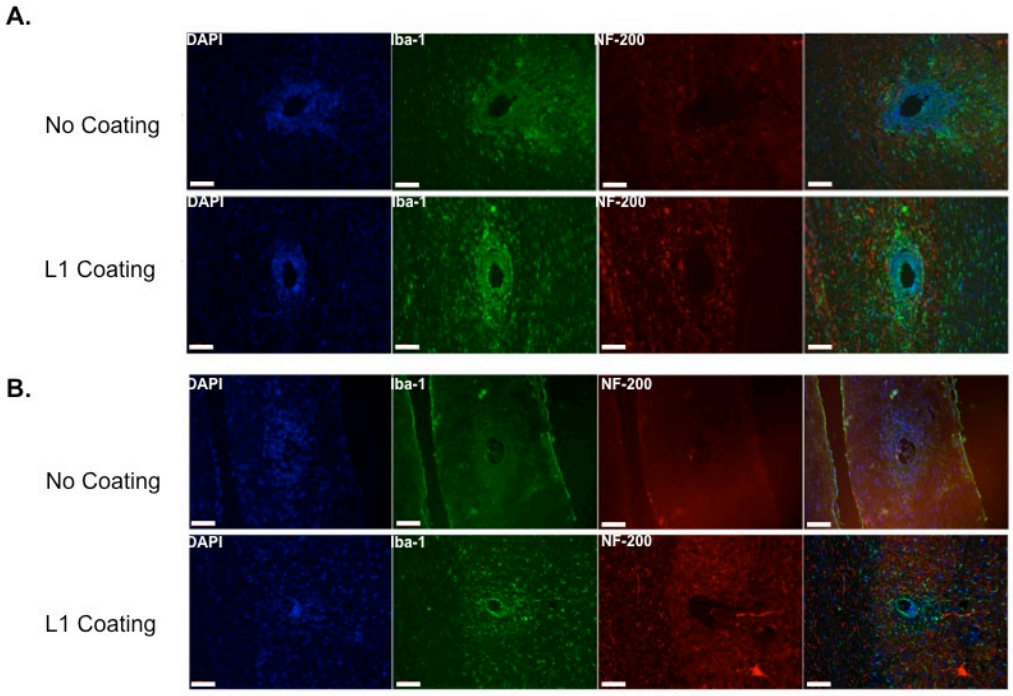


**Figure 2.2**. Immunofluorescence images of rat SC around uncoated and L1-coated electrodes. **A**: After 1 week, Iba-1 staining was decreased in L1 coated electrodes. **B**: After 4 weeks, this differences was more pronounced. Scale bar represents 100 µm.

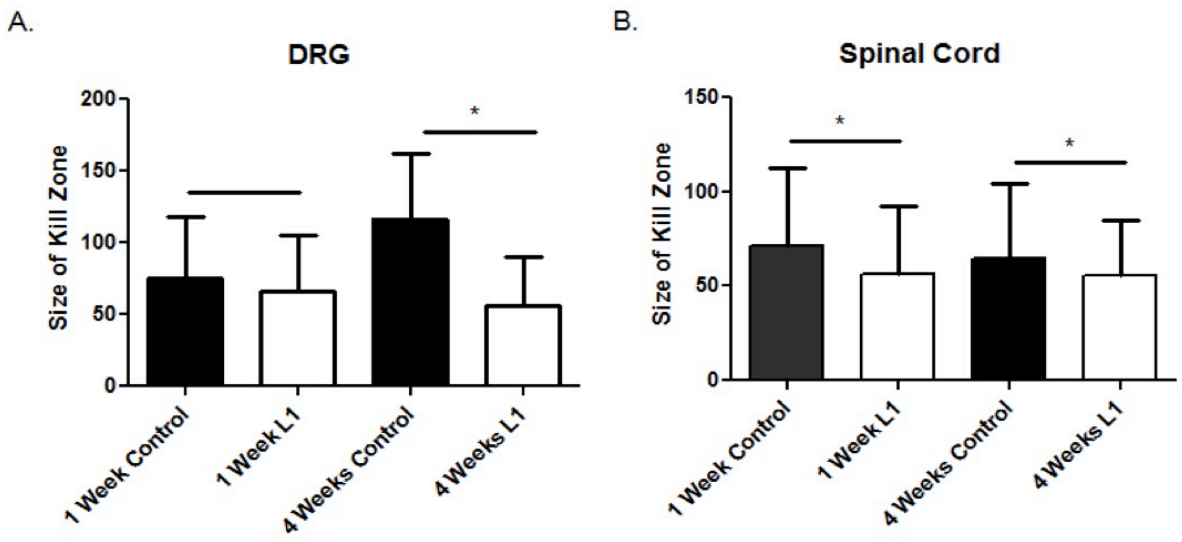


**Figure 2.3**. NF-200 analysis of the kill zone in DRG (**A**) and SC (**B**). **A**: In the DRG, uncoated electrodes ($n$ = 4 at 1 week; $n$ = 3 at 4 weeks) had significantly larger kill zones than L1 coated electrodes ($n$ = 4 at 1 week; $n$ = 3 at 4 weeks). **B**: In the SC, uncoated electrodes ($n$ = 5 at 1 week; $n$ = 3 at 4 weeks) electrodes had significantly larger kill zones than L1 coated electrodes ($n$ = 6 at 1 week; $n$ = 5 at 4 weeks). *$p < 0.05$; error bars represent mean + standard deviation.

coating decreases inflammation and promotes neuronal health around the implantation site.

Results were quantified using a custom-written MATLAB program (The Mathworks, Inc., Natick, MA) with a graphic user interface (GUI) to measure pixel intensity for images taken using the same exposure time. The results of this analysis for quantification of the kill zone are provided in Figure 2.3 and detail differences in both the DRG and SC tissues at both time points. For NF-200 analysis, the location of the implant was defined using the nuclear stain and then the distance to the edge of the kill zone determined (Figure 2.3). The average kill zone size was determined for each implant and the mean kill zone size reported for each group. In both DRG and SC, the size of the kill zone was significantly decreased in the presence of the L1 coating. For Iba1 analysis, a plot of the intensity (y-axis) versus the distance from the implant site (x-axis) was established by outlining the location of the implant and then comparing the intensity of Iba1 staining to a background image (taken of tissue far from the implant site) (data not shown). These curves will be used to calculate the rate of decay of Iba-1 staining (ongoing).

Finally, to characterize the non-Iba-1, non-NF-200 and non-GFAP positive cells around the electrode implantation site, vimentin and S100 were used to identify fibroblasts and Schwann cells, respectively. Figure 2.4 depicts this staining combination in the rat DRG at both 1 and 4 week time points. While the vimentin staining is similar when uncoated and coated electrodes are compared, the S100 staining appears more evenly distributed and less disrupted with the L1 coating. L1 has been shown to impact Schwann cell differentiation and myelination [2, 3], and this observation indicates that the L1 coating may benefit this important cell type as well.

***Result 2: Development and characterization of PEDOT/carbon nanotube (CNT) coating***

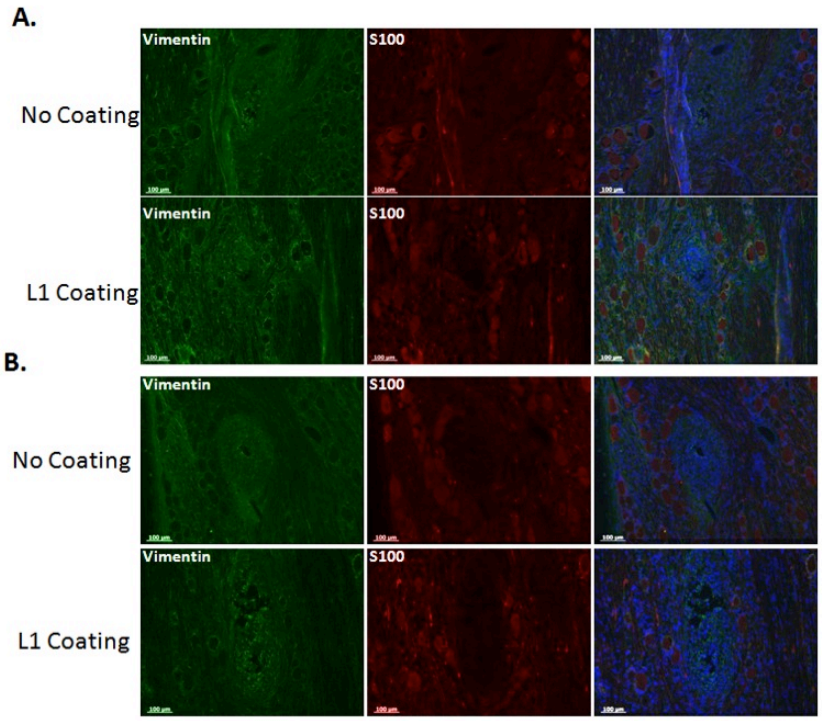


**Figure 2.4**. Immunofluorescence images of vimentin (green) and S100 (red) staining of rat DRG around uncoated and L1-coated electrodes after 1 week (**A**) and 4 weeks (**B**).

The function and longevity of implantable microelectrodes depend heavily on the electrode materials, which need to be highly stable and biocompatible. While conducting polymers have been coated on microelectrodes for neuronal stimulation and recording, and have been shown to be potentially promising, their practical applications have been limited due to unsatisfying stability under stimulation[5]. We have tried to improve the stability of poly(3,4-ethylenedioxythiophene) (PEDOT) for neural stimulation by introducing carbon nanotubes (CNTs) into the polymer. PEDOT doped with pure carbon nanotubes can be electrochemically deposited on Pt microelectrodes to form a uniform coating, as shown in Figure 2.5a. We found that the PEDOT/CNT coated Pt microelectrodes exhibited much higher charge capacity than the bare electrode (Figure 2.1c), and the coatings could decrease the electrode impedance by 1-2 orders. In addition, the PEDOT/CNT coated electrode exhibited a high charge injection limit of about 2.5 $mC/cm^2$.

We also investigated the stability of the PEDOT/CNT coatings during various stimulation conditions. In the first test, the electrodes were stimulated in phosphate buffer saline (PBS, 10 mM, pH 7.4) using CV from -0.9 to 0.5 V, at a scan rate of 100 mV/s for 3000 cycles (about 24 hours). After this strong stimulation, there are no cracks or detachment of the PEDOT/CNT coating, even in its microstructure (Figure 2.5B). Next, To better simulate the stimulation conditions for practical application and test the long-term stability, the PEDOT/CNT coated electrodes were soaked in PBS for three months, and between the week 5 and 7 they were stimulated using a clinically relevant neural stimulation protocol (a biphasic, charge balanced

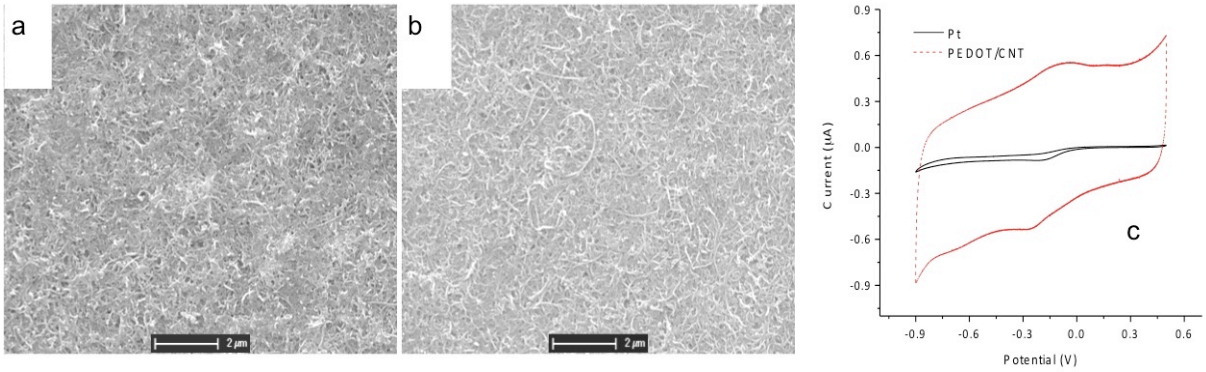


Figure 2.5. SEM images of the PEDOT/CNT coating on microelectrode before (a) and after (b) electrical stimulation. (c) Cyclic voltammatry comparison of PEDOT/CNT coated and bare Pt microelectrodes. fluorescent image, the scale bar represents 100 μm.

pulse current at 1 mC/cm2 at 50 Hz) for two weeks. Figure 2.6A shows representative plots of electrode impedance change over time during the three months' soaking in PBS for different electrodes. Both of the stimulated and un-stimulated normal PEDOT/CNT coated electrodes have much lower impedance than bare Pt electrodes, and their impedance remains unchanged over the three-month period. This result is in good agreement with the morphology examination which shows the PEDOT/CNT coatings are highly stable. For some of the ultrathin PEDOT/ CNT film coated electrodes, their impedance may increase a little bit after the electrical stimulation, which may be ascribed to the fact that the CNT networks that offer the polymer mechanical strengthen is not well formed as the coatings are too thin.

In order to test the biocompatibility of the PEDOT/CNT, it was electrochemically coated on gold sputtered cover slips, and the resulted PEDOT/CNT coated cover slips were used as substrates for neuron culture. As shown in Figure 2.6B is the fluorescent image of neurons grown on the PEDOT/CNT surface. It is clear that the neurons grown evenly over the whole PEDOT/ CNT coating, and neurite networks were well established, which indicate that neurons grown

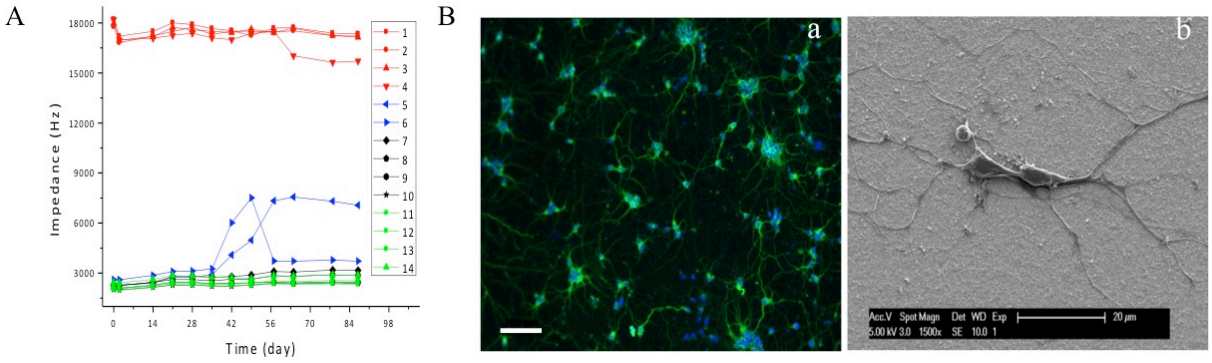


Figure 2.6. (A) Monitored electrode impedance changes at 1K Hz over time during the three-month soaking in PBS. Plots 1-4 in red are bare Pt electrodes; plots 5-6 in blue are ultrathin PEDOT/CNT (deposition charge less than 5 μC) coated Pt electrodes with stimulation; plots 7-10 in black and plots 11-14 in green are normal PEDOT/CNT (deposition charge more than 10 5 μC) coated Pt electrodes with (7-10) and without (11-14) stimulation. (B) Fluorescent (a) and SEM (b) images of neurons grown on PEDOT/CNT surfaces. For the fluorescent image, the scale bar represents 100μm.

healthily on the PEDOT/CNT substrate. Further characterization was carried out with SEM, as shown in Figure 2.6B. As can be seen, the neurons attached tightly to the PEDOT/CNT surface, and the long neurite extensions were spread out. These results suggest that PEDOT/CNT supports healthy cell attachment and neurite outgrowth, implying that the PEDOT/CNT possess a good biocompatibility with neurons.

***Plans:*** We have completed the passive electrode/tissue interface evaluations and the L1 coating. We plan to write and submit one manuscript on results obtained. Next stage of the project will be focused on active stimulation electrodes. We plan to evaluate the effects of chronic stimulation on electrodes implanted into the rat DRG. For these studies, a total of 24 animals (6 groups of 4 animals) will be used to test the effect of daily stimulation for either 7 or 28 days. Stimulation parameters will be modeled after those utilized by McCreery *et al*. [4]. The tissue reaction around PEDOT/carbon nanotubes (CNTs) coating and PEDOT/CNT/ Dexamethasone will be evaluated and compared to uncoated Pt/Ir electrodes.

### *Project 3. Virtual reality environment for prosthetic training and testing*

#### *Objectives*

A virtual environment will be created that will allow amputees to: 1) test simulated neuroprosthetics and control algorithms, and 2) practice using the neuroprosthetic in a virtual training environment. The main objective for the FY06 funding period is to design, acquire, and assemble a virtual reality system for training people to use an upper extremity neuroprosthesis (months 1-6). In months 3-12, we will develop and test the VR system with myoelectric control inputs, and test the system with upper extremity amputees performing simulated reaching tasks.

In FY07 we will further refine our VR training system and optimize the use of myoelectric signals for controlling specific natural tasks for which they may be best suited, natural grasping and pinching movements. In addition, we will use direct brain interface (DBI) signals, such as magnetoencephalography (MEG) and electrocorticography (ECoG) to control a virtual hand. We will also explore how these signals can be used interactively with EMG signals. The ultimate goal is to develop a DBI or hybrid EMG-DBI system that persons with high-level spinal cord injury can use to regain motor function.

#### *Results*

**Approval from both the U.S. Army HRPO and University of Pittsburgh IRB**

We have successfully secured approval from both the Army Human Research Protection Office (HRPO) and the University of Pittsburgh Institutional Review Board (IRB) to conduct human studies in both able-bodied individuals and individuals with limb amputations. One control subject was recruited in this study and preliminary data analysis is being done to evaluate the effectiveness of the paradigm. Thereafter further recruitment will take place. Our protocol was renewed successfully by the University of Pittsburgh IRB for the year 2011.

**Fully-functional virtual reality (VR) simulator system for prosthetic control training**

A fully-functional virtual reality simulator using a combination of BCI2000 software and the MATLAB/SIMULINK Virtual Reality Toolbox was developed previously. This VR environment included an artificial hand that grasped or pinched virtual objects. We have further developed this virtual reality environment using advanced virtual reality environment tool namely, Unity3d as shown in Fig. 3.1. This is discussed in the following section.

**Developed advanced virtual reality environment**

VR technologies have been used reliably in healthcare for more than a decade (Moline 1997, Sear et al. 2008). In particular, in rehabilitation, VR enables the impaired individuals to perform the tasks not otherwise available to them. The VR games can "amplify" the residual hand movement and render a full-range virtual hand movement for grasping various virtual objects in order to motivate the individual in rehabilitation training. Essentially, the VR game can ensure that the task difficulty matches the skill level and keeps the individual in progressing towards faster recovery. Also, during such

functional recovery, VR paradigms can provide quantitative assessment of the progress of patient's rehabilitation in fine scales. Inspired by the growing demand for virtual reality gaming applications in rehabilitation, we have improved our previously developed virtual reality environment into behaviorally rich virtual environment as shown below in Fig. 3.1(B). In this virtual environment a virtual avatar will represent the participating subject in the virtual world. This avatar is human like, in the sense that, he has all the degrees of freedom as humans in terms of bilateral arm and hand movements. By controlling this avatar and thus empathizing with the


Figure 1 A virtual avatar will reach and grasp objects in virtual environment as shown here. The objects are designed such that grasping (ball, hammer) and pinching (pen) actions of the hand can be emulated in virtual environment. This environment was created in Unity3d.

avatar, subjects get a real world experience in the virtual world. This virtual reality environment was developed in Unity3D (www.unity3d.com).

**Preliminary data analysis**

One control subject has participated in this virtual reality task. The task began with the subject controlling three synergies, including grasp and pinch synergies, with three muscle activities recorded electromyographically (EMG) from three muscles namely flexor digitorum profundus, biceps and trapezius, all on the same arm. The surface EMG signals were recorded using digital amplifiers (g.tech). After initial training, once the subject gained independent control of the synergies, the subject is presented with desired postures, where he/she will need to combine the muscle activities, thereby combining the synergies to achieve the desired posture. Thus by controlling just three synergies/movement primitives subject successfully performed 15 different hand postural movements. Figure 3.2 shows three surface-electromyogrpahic signals recorded from a control subject (Subject A) who commanded three synergies which in turn controlled the hand posture of a virtual hand. As the desired hand posture (bottom plot) changed, Subject A used different combinations of synergies to achieve the desired hand posture.

**A working model of real-time MEG software**

We have a working model of real-time MEG (rtMEG) software that works for Elekta Neuromag system. The flow of the signals is illustrated in Figure 3.3. The Acquisition computer controls the acquisition, stores the data and runs the rtMEG interface. Another computer drives the experimental paradigm by providing stimuli to the subject and sending trigger events that eventually go to the MEG data file. The rtMEG interface writes data to the Fieldtrip buffer,

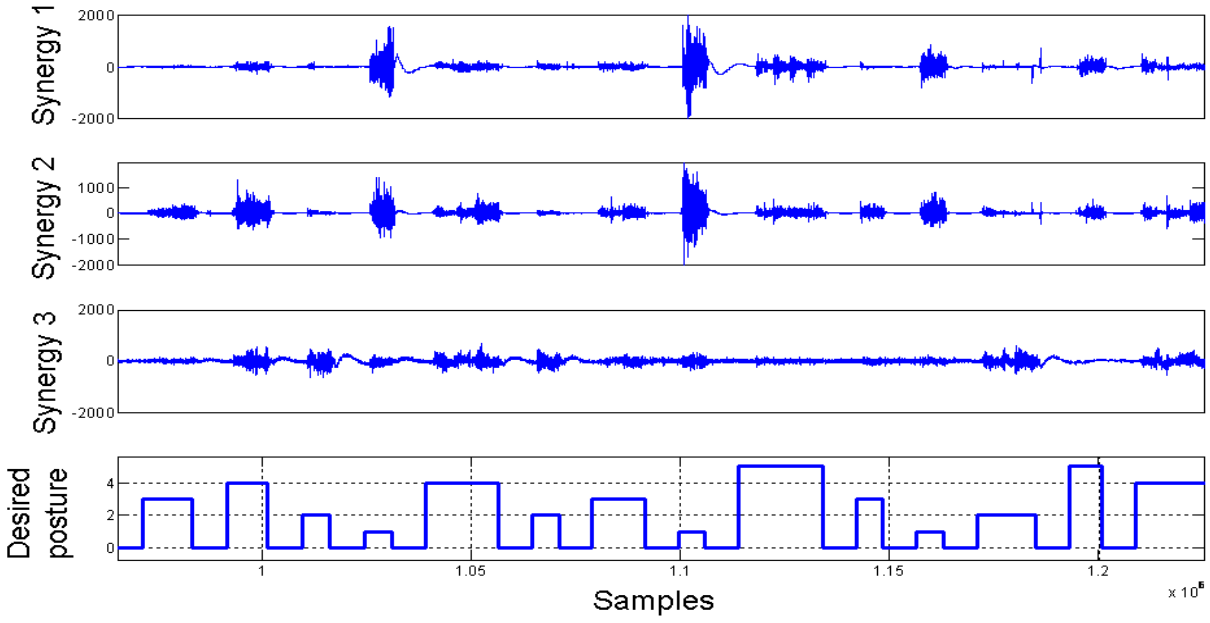


Figure 3.2 Three surface-electromyographic signals recorded from a control subject (Subject A) command three synergies which in turn control the hand posture of a virtual hand. As the desired hand posture changes, Subject A uses different combinations of synergies to achieve the desired hand posture.

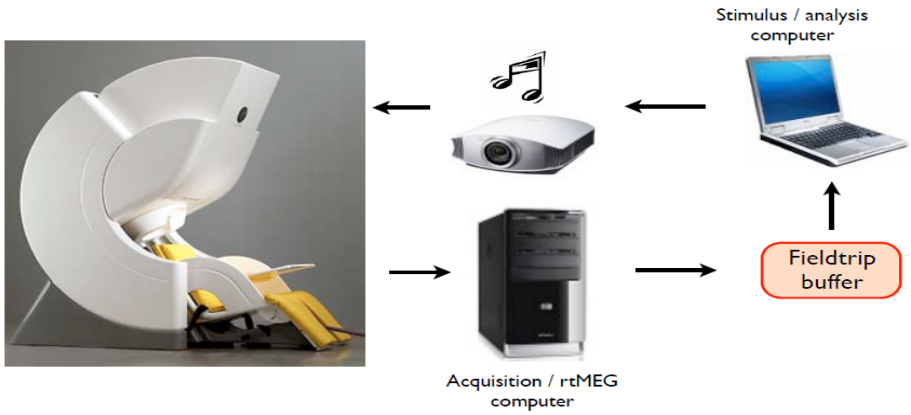


Figure 3.3 Illustration of a typical setup with rtMEG. The Acquisition computer controls the acquisition, stores the data and runs the rtMEG interface. Another computer drives the experimental paradigm by providing stimuli to the subject and sending trigger events that eventually go to the MEG data file. The rtMEG interface writes data to the Fieldtrip buffer, which can be run by rtMEG or by any other computer in the network. The application(s) reading from this buffer can run on the stimulus computer or on any other computer connected in the network.

which can be run by rtMEG or by any other computer in the network. The fieldtrip buffer can be accessed by any routine that runs on any computer in the network. Here to demonstrate the

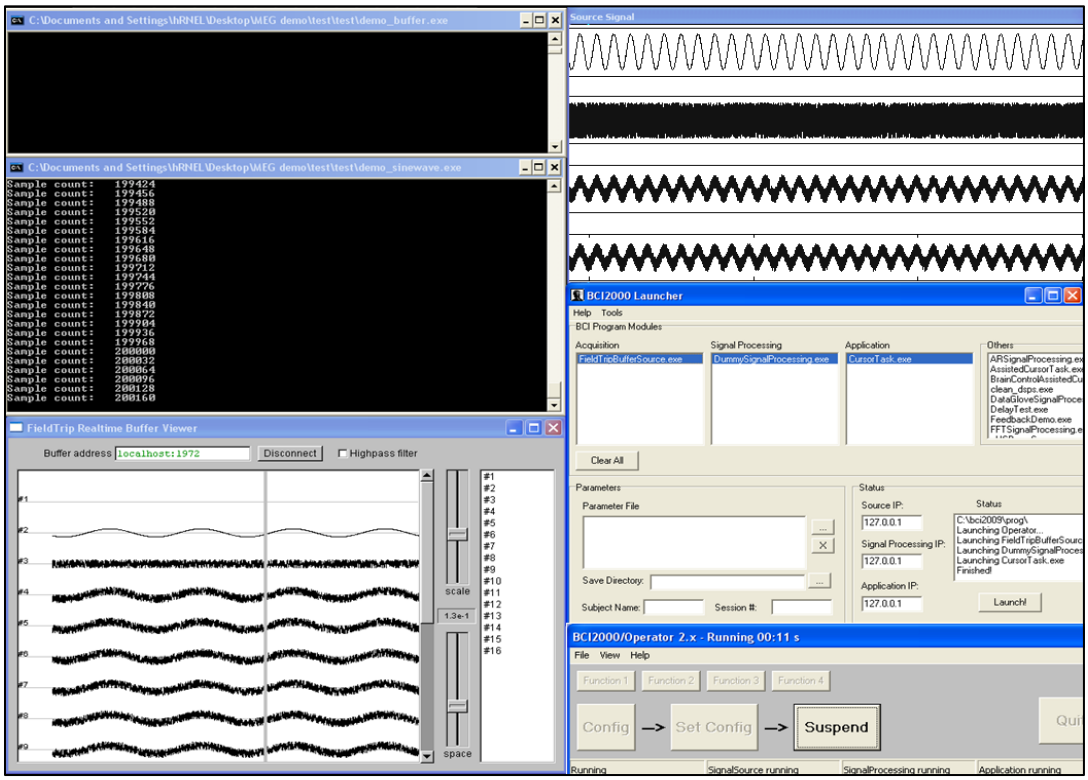


Figure 4 On the left hand side are the simulated sine wave signals (with additional noise) being sent to the field trip buffer. One the right hand side, is a general purpose BCI software (BCI2000) reading the field trip buffer in real time. Bottom left corner plot indicates the signals being sent and top right corner plot shows the signals recorded.

functionality of rtMEG we have used BCI2000, a general purpose BCI software to read from the fieldtrip buffer. The results are as shown in the Figure 3.4.

***Plans***

1. Providing a rewarding gaming environment seemed to have increased the level of motivation of the subjects in studies reported previously. A game like environment is being developed where Subjects can control avatars (male/female) depending on Subjects to grasp and reach virtual objects and win rewards on their way to final level in a VR game.
2. The mathematical algorithms such as online classifiers and real-time dimensionality reduction algorithms that run behind the scenes are being embedded into LabView. LabView will then communicate with Unity3d (Figure 1). This is a work in progress.
3. rtMEG is near completion and fully functional by itself. The virtual reality environment developed in Unity3d needs to be integrated with rtMEG to provide a real time paradigm in MEG setup.

### *Project 4.* Prosthetic hardware testing

#### *Objectives*

Little objective or validated information exists about the quality and functional reliability of prostheses. The primary objective for the FY06 funding period is to develop and assemble a testbed for life-cycle testing of a variety of prosthetic feet. In months 1-6, we will design the testing apparatus and acquire and assemble the hardware and software for testing. We will also complete pilot testing with a small number of prosthetic limbs to validate the system.

In FY07, we will use the testbed to perform life-cycle testing of a variety of prosthetic feet. In months 1-6, we will acquire representative samples of the most popular foot designs and create fixturing for attaching the feet to the testbed. In months 3-12, we will perform the life-cycle testing and analyze the data.

#### *Results*

Acquire prosthetic feet and completed pilot testing: Prosthetic feet from three different manufacturers was ordered. The feet being tested are as follows: three Freedom 1000 Sierras, three Ossur Reflex VSPs, and three Ohio Willow Wood Pathfinders (Table 1). Technical issues with the machine were resolved and pilot testing with a Freedom 1000 Sierra was completed. Pilot testing was done on actual specimens; starting with a Freedom 1000 Sierra at P3 loading level. This first test was completed successfully. Other feet will be tested at the P5 loading level. During the testing, position and force data was collected for each channel (heel and forefoot). This data will allow us to compare feet on the basis of stiffness and creep, along with pass and fail. A data analysis program was developed to calculate these parameters.

Procurement: All prosthetic feet from the three different manufacturers were received including Freedom FS Sierras, Ossur VSPs, and Ohio Willow Wood Pathfinder II. Teflon sheets and Teflon tape were also purchased. Teflon was used on the bottom of the loading surface of the plates on both actuators so that load application at foot was frictionless.

Testing with P5 loading level: During the static proof tests, a maximum force of 2240 N is applied in a downward direction for 30 seconds on the heel and forefoot consecutively. During the ultimate strength tests, force is applied separately on the heel and forefoot, increasing gradually from 3360N to 4480 N at the rate of 175N/ 20 seconds. During the fatigue tests, load is applied on both the heel and forefoot alternatively for 2,000,000 cycles at a frequency of 1 Hz followed by a final static proof test at the P5 loading level. Each foot is examined before and after every test and often during the fatigue test.

**Results**: ISO 10328 testing at the P5 loading level has been completed on all nine feet without any failures. One Pathfinder II failed under suspicious circumstances during the fatigue test, so a replacement specimen was tested. This replacement Pathfinder II passed all the tests, so the previous foot was excluded from any subsequent analysis.

Figure 4.1: Freedom Sierra FS1

**Table 4.1: Characteristics of prosthetic feet tested**

| Manufacturer | Model | Activity level | size | Material | category | Weight limit |
|---|---|---|---|---|---|---|
| Freedom | Sierra FS1 | High | 26 cm | Carbon fiber | 9 | 365lbs |
| Ohio Willow Wood | Pathfinder II | High | 26 cm | Carbon fiber& pneumatic heel spring | 9 | 350 lb |
| Ossur | Re-flex VSP | High | 26 cm | Carbon fiber &compression spring | 9 | 365lbs |

High activity level include rigorous activity, competitive sports, running, power lifting, and snowboarding.

Figure 4.2: Ossur VSP

Figure 4.3: Ohio Willow Wood Pathfinder II

**Table 4.2: Test Results**

| Prosthetic Foot | Proof Test | Ultimate Test | Fatigue Test | Post-Fatigue Proof Test |
|---|---|---|---|---|
| Freedom Sierra 1 | Pass | Pass | Pass | Pass |
| Freedom Sierra 2 | Pass | Pass | Pass | Pass |
| Freedom Sierra 3 | Pass | Pass | Pass | Pass |
| Ossur VSP 1 | Pass | Pass | Pass | Pass |
| Ossur VSP 2 | Pass | Pass | Pass | Pass |
| Ossur VSP 3 | Pass | Pass | Pass | Pass |
| OWW Pathfinder II 1 | Pass | Pass | Pass | Pass |
| OWW Pathfinder II 2 | Pass | Pass | Pass | Pass |
| OWW Pathfinder II 3 | Pass | Pass | Pass | Pass |

Stiffness and creep at the heel and forefoot was calculated for each specimen during the pre- and post-fatigue proof tests. Stiffness was calculated by taking the slope of the loading portion of the force-displacement curves. Creep was determined by taking the difference in displacements between the beginning and end of the proof tests. The results of which can be seen in the figures below:

**Figure 4.4: Forefoot Stiffness Results**

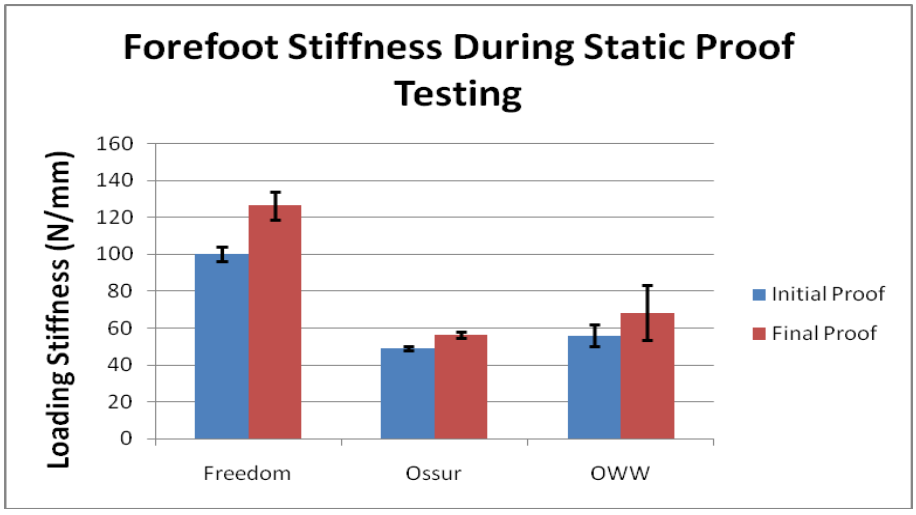


**Figure 4.5: Heel Stiffness Results**

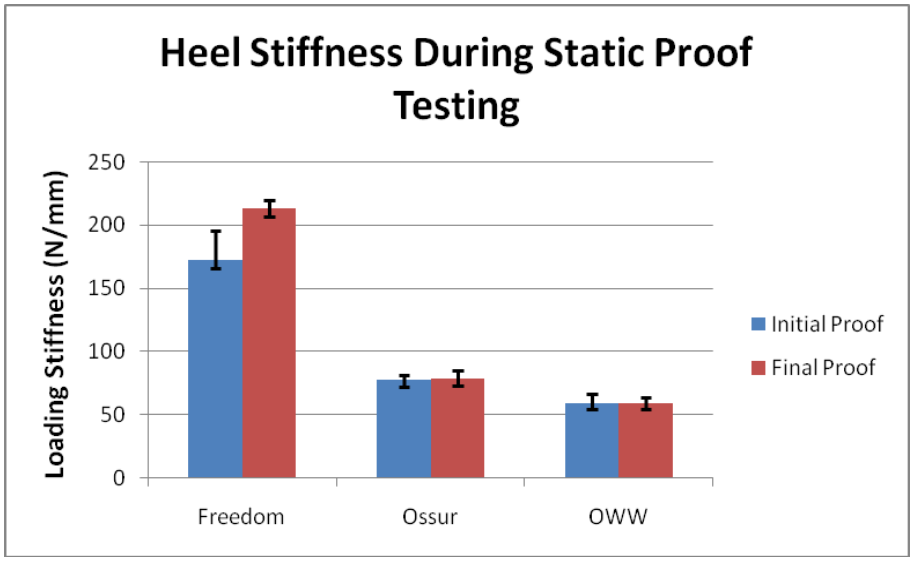


**Figure 4.6: Forefoot Creep Results**

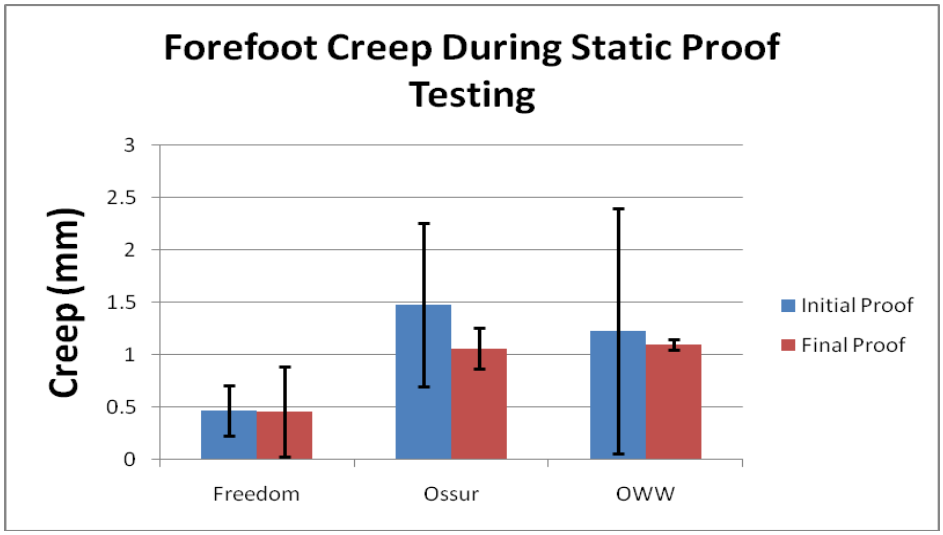


**Figure 4.7: Heel Creep Results**

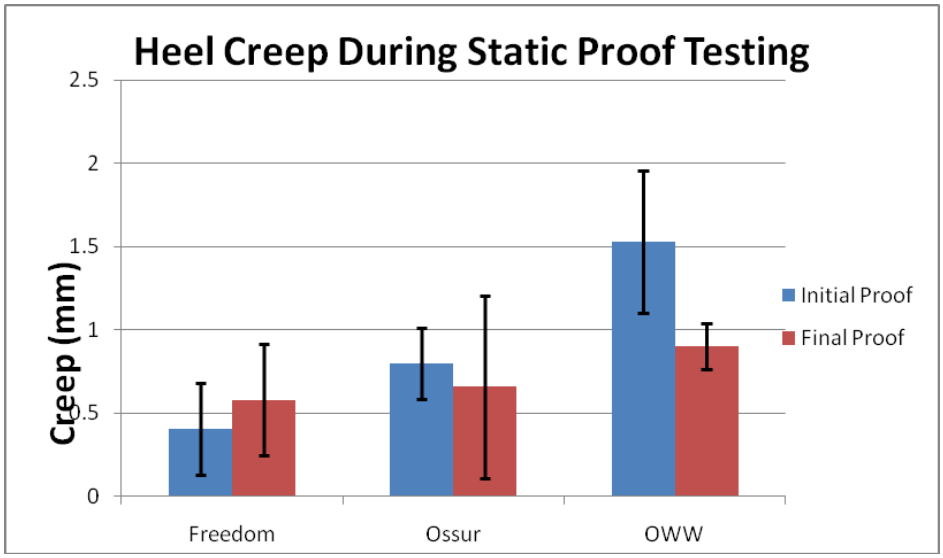


A Kruskal-Wallis test, with the significance level adjusted to 0.025 with Bonferroni's correction for multiple comparisons, was applied to the data to determine any differences between the models of feet and pre- and post-fatigue behavior. While trends indicated that the Freedom feet are more stiff and creep less, no statistically significant differences were found.

***Plans:***

Now that testing on all nine prosthetic feet is complete, the data is being analyzed and prepared for submission to a scientific journal. Since no failures occurred during the ISO testing of the feet, more rigorous tests will be developed in order to simulate the failures that clinicians and prosthetic users experience in the field. This will include developing tests that investigate the behavior of the feet under torsional loads and abnormal environmental conditions, such as excessive heat and cold.

**Key Research Accomplishments in last year**

***Project 1. Develop a somatosensory neural interface (SSNI)***

| Milestones | Progress |
|---|---|
| Afferent microstimulation and cortical recording experiments | • Computational model of PAMS in DRG has been developed and validated. A full length paper is in review by the Journal of Neural Engineering.<br>• Computational model reveals a surprising bias favoring recruitment of medium diameter fibers (Figures 1.2-1.4). The strength of this bias was underestimated in previous in vivo studies, but is important for ensuring selective stimulation of the full range of sensory fiber types supporting touch and proprioception. In particular, the medium diameter sensory fibers of interest include group II muscle spindle afferents needed for joint position sense and several cutaneous afferent neurons which convey tactile sensations (Figure 1.2-1.4).<br>• Primary afferent microstimulation (PAMS) evokes 'proprioceptive' neuronal responses in the brain that are similar to those evoked by movement of the leg and increasing the intensity or rate of stimulation enhances the proprioceptive responses in the brain (Figure 1.5).<br>• Evaluation of fundamental features of stimulation reveal that stimulation pulse rate and intensity have dramatic effects on the response of neurons in S1 (Figure 1.6). |
| Chronic stimulation and recording experiments | • Animal protocol approved by Pitt IACUC and Army ACURO. Chronic experiments will start in Spring, 2011. |

***Project 2. Establishment of Neural interface stability and optimization***

| **Milestones** | **Progress** |
|---|---|
| Microelectrode array implant surgeries with treated and untreated electrodes. | • Completed the implantation of L1 treated and untreated parylene C insulated electrodes. |
| Histological evaluation of implant sites | • Completed the tissue response evaluation for the untreated and L1 treated electrodes implanted acute and chronically in DRG and spinal cord. |
| Implant surgeries for tissue reaction to chronic stimulation study. | • Developed PEDOT/CNT and PEDOT/CNT/Dexamethasone coatings for the stimulation electrodes. Prototype implants have been made. The animal implantation is ready to go. |
| Histological evaluation of implant sites | Not started. |

***Project 3. Utilization of a virtual reality environment for prosthetic training and testing***

| Milestones | Progress |
|---|---|
| Developing advanced virtual environment | Completed |
| Integrate complex mathematical algorithms into Virtual Reality Environment | In Progress |
| Recruiting Control subjects | In Progress |
| Testing and validation of VR environment | In Progress |
| Refine VR system and test the system with amputees | • We have renewed our protocol with the Institutional Review Board (IRB) at the University of Pittsburgh for the year 2011.<br>• We have refined the existing basic VR environment to advanced VR environment with an avatar that can reach and grasp virtual objects.<br>• We would like to thoroughly test our refined VR systems in non-impaired individuals before we start recruiting individuals with upper extremity amputation. |
| Use direct brain interface signals to control virtual arm; integrate DBI and EMG for control. | • MEG component was successfully included into the VR study.<br>• rtMEG needs to be integrated with the advanced virtual reality environment. |

***Project 4. Prosthetic hardware testing***

| **Milestones** | **Progress** |
|---|---|
| Design and assemble system for prosthetic life-cycle testing. | • Complete |
| Develop data acquisition system and complete pilot testing | • Complete |
| Acquire prosthetic feet and develop fixturing for life-cycle testing | • Complete |
| Complete testing of prosthetic feet. | • Complete |
| Data analysis and preparation of journal paper submission | • Ongoing |
| Develop fixture for torsional testing of prosthetic feet | • Ongoing |

## REPORTABLE OUTCOMES

### *Project 1. Develop a somatosensory neural interface (SSNI)*


1. Wagenaar JB, Ventura V, Weber DJ (2011) State-space decoding of primary afferent neuron firing rates. J Neural Eng 8:016002.
2. Rigosa J, Weber DJ, Prochazka A, Stein RB, Micera S. (2010) Neuro-fuzzy decoding of sensory information from ensembles of simultaneously recorded dorsal root ganglion neurons for FES applications. J Neural Eng. Accepted pending revisions.
3. Ayers CA, Gaunt RA, Hokanson JA, Weber DJ (2010) Primary somatosensory cortex responses to simple patterns of primary afferent microstimulation in L6/L7 dorsal root ganglia of anesthetized cats. Program No 29515 2010 Neuroscience Meeting Planner San Diego, CA: Society for Neuroscience, 2010 Online.
4. Bourbeau DJ, Hokanson JA, Rubin JE, Ermentrout GB, Weber DJ (2010) A computational model for simulating recruitment of peripheral nerve fibers by intraneural microstimulation. Program No 38314 2010 Neuroscience Meeting Planner San Diego, CA: Society for Neuroscience, 2010 Online
5. Bruns TM, Gaunt RA, Simpson TW, Weber DJ (2010) Primary afferent neural activity recorded with non-penetrating electrodes on lumbar DRG surface. Program No 29516 2010 Neuroscience Meeting Planner San Diego, CA: Society for Neuroscience, 2010 Online.
6. Hokanson JA, Ayers CA, Gaunt RA, Weber DJ (2010) Novel stimulation paradigm to provide somatosensory feedback in a neural prosthesis. Program No 29512 2010 Neuroscience Meeting Planner San Diego, CA: Society for Neuroscience, 2010 Online
7. Wagenaar JB, Hokanson JA, Ayers CA, Weber DJ (2010) Development of an efficient data-management system in Matlab. Program No 20912 2010 Neuroscience Meeting Planner San Diego, CA: Society for Neuroscience, 2010 Online

***Project 2. Establishment of Neural interface stability and optimization***

1. Xiliang Luo and Xinyan Tracy Cui, Electrochemical deposition of conducting polymer coatings on magnesium surfaces in ionic liquid, Acta Biomateriala, Sep 2010, PMID: 20832505
2. Erdrin Azemi, Carl Lagenaur and Xinyan Tracy Cui, The Surface Immobilization of the Neural Adhesion Molecule L1 on Neural Probes and its Effect on Neuronal Density and Gliosis at the Probe/Tissue Interface, Biomaterials, Oct 2010, PMID: 20933270
3. X.T.Cui, Characterization and Improvement of Neural Electrode-Tissue Interface, Microscopy and Microanalysis (2010), 16: 1024-1025
4. X. Luo, C. Matranga, S. Tan, N. Alba, X. T. Cui, Carbon Nanotube Based Capsules for the Controlled Loading and Release of Drugs, submitted to *SMALL*
5. William R Stauffer, Pak-ming Lau, Guo-qiang Bi, X. Tracy Cui, Rapid Modulation of Local Neural Activity by Electrically Controlled Drug Release from Conducting Polymer-coated Microelectrodes, submitted to *Journal of Neural Engineering*
6. Michael S. Freedman and Xinyan Tracy Cui, Substrate Electrode Morphology Affects Electrically Controlled Drug Release from Electrodeposited Polypyrrole Films, submitted *Solid State Electrochemistry*
7. Erdrin Azemi, Shawn Sapp, Silvia Luebben, X.T.Cui, Improving Neural Implant Biocompatibility via Biomimetic Design, Material Research Soceity Spring Meeting, Symposium JJ "Stretchable electronics and conformal biointerfaces", San Francisco, CA, April 2010
8. X.T.Cui, Improving Neural Implant Biocompatibility via Biomimetic Surface Design, 2nd International Conference on Neuroprosthetic Devices (ICNPD 2010), Beijing, China, February 2010
9. X. T. Cui, Improving Neural Implant Biocompatibility via Biomimetic Design, Biomedical Engineering Society Annual Meeting to be held in Austin, Texas on October 6-9, 2010

***Project 3. Utilization of a virtual reality environment for prosthetic training and testing***

Journal papers

Guo C, Li X, Taulu S, Wang W, Weber DJ (2010) Real-time robust signal space separation for magnetoencephalography. IEEE Trans Biomed Eng 57:1856-1866.

Wang W, Sudre GP, Kass RE, Collinger JL, Degenhart AD, Bagic AI, Weber DJ (2010) Decoding and cortical source localization for intended movement direction with MEG. Journal of Neurophysiology 104: 2451-2461.

Vinjamuri R, Weber DJ, Mao Z-H, Collinger JL, Degenhart AD, Kelly JW, Boninger ML, Tyler-Kabara EC, Wang W (In Review) Towards synergy based brain machine interfaces. IEEE Trans Biomed Eng.

Xu Y, Sudre G, Wang W, Weber DJ, Kass R (In Review) Characterizing global statistical significance of spatio-temporal hot spots in MEG/EEG source space via excursion algorithms. Statistics in Medicine.

Degenhart AD, Kelly JW, Ashmore RC, Collinger JL, Tyler-Kabara EC, Weber DJ, Wang W (In press) Craniux: a LabVIEW-based modular software framework for brain-machine interface research. Comput Intell Neurosci.

Sudre GP, Parkkonen L, Bock E, Sylvain B, Wang W, Weber, DJ (In Review) rtMEG: a real-time software interface for magnetoencephalography. Comput Intell Neurosci.

Zhang J, Sudre G, Li X, Wang W, Weber D, Bagic A (In press) Group independent linear discriminant analysis for magnetoencephalography-based brain computer interfaces. IEEE Trans Neural Syst Rehab Engr.

Peer reviewed conference papers

Vinjamuri R, Sun M, Weber D, Wang W, Crammond D, Mao Z-H (2009) Quantizing and characterizing the variance of hand postures in a novel transformation task. In: IEEE EMBC. Minneapolis, MN.

Sudre, G., Wang, W., Song, T., Kajola, M., Vinjamuri, R., Collinger, J., et al. (2010). rtMEG: A Real-Time Software Toolbox for Brain-Machine Interfaces Using Magnetoencephelography. 17th International Conference in Biomagnetism, 1-4.

Abstracts

Vinjamuri R, Weber DJ, Mao Z-H, Collinger JL, Degenhart AD, Kelly JW, Boninger ML, Tyler-Kabara EC, Wang W (2010) Towards synergy based brain machine interfaces. Proceedings of the Society for Neuroscience Annual Meeting; 2010; San Diego, CA.

Degenhart AD, Collinger JL, Vinjamuri R, Kelly JW, Tyler-Kabara EC, Weber D, Wang W (2010) Classification of hand posture from electrocorticographic signals recorded during varying force conditions. Proceedings of the Society for Neuroscience Annual Meeting; 2010; San Diego, CA.

***Project 4. Prosthetic hardware testing***

A poster was presented on "Protocol Development for Prosthetic Feet Testing Standards" at State of Science Symposium on Regenerative Rehabilitation at Walter Reed Army Medical Center. Many clinicians and prosthetic professionals were curious to know the outcome of this study. Another paper was submitted on "Mechanical Testing of Heavy Duty Prosthetic Feet" for RESNA 2010 conference proceedings. This paper was descriptive in the nature including preliminary analysis of present result.

1. **Kumar A, Pearlman J, Mason Z, Hong EK, Laferrier J, Cooper R and Cooper RA.** Development of Protocol for Prosthetic Feet Testing Standards. In: State of Science Symposium on Regenerative Rehabilitation at Walter Reed Army Medical Center November 13, 2009

2. **Kumar A, Pearlman J, Mason Z, Karmarkar A, Cooper R and Cooper RA**. Mechanical Testing of Heavy Duty Prosthetic Feet. Submitted manuscript for RESNA 2010 Annual Conference.